

## Discovery of a long-lived low-lying isomeric state in $^{80}\text{Ga}$

B. Cheal,<sup>1,\*</sup> J. Billowes,<sup>1</sup> M. L. Bissell,<sup>2</sup> K. Blaum,<sup>3</sup> F. C. Charlwood,<sup>1</sup> K. T. Flanagan,<sup>4</sup> D. H. Forest,<sup>5</sup> S. Fritzsche,<sup>6,7</sup> Ch. Geppert,<sup>6,8</sup> A. Jokinen,<sup>9,10</sup> M. Kowalska,<sup>3,11</sup> A. Krieger,<sup>8</sup> J. Krämer,<sup>8</sup> E. Mané,<sup>1</sup> I. D. Moore,<sup>9,10</sup> R. Neugart,<sup>8</sup> G. Neyens,<sup>2</sup> W. Nörtershäuser,<sup>6,8</sup> M. M. Rajabali,<sup>2</sup> M. Schug,<sup>3</sup> H. H. Stroke,<sup>12</sup> P. Vingerhoets,<sup>2</sup> D. T. Yordanov,<sup>3</sup> and M. Žáková<sup>8</sup>

<sup>1</sup>*School of Physics and Astronomy, The University of Manchester, Manchester M13 9PL, United Kingdom*

<sup>2</sup>*Instituut voor Kern- en Stralingsfysica, Katholieke Universiteit Leuven, B-3001 Leuven, Belgium*

<sup>3</sup>*Max-Planck-Institut für Kernphysik, D-69117 Heidelberg, Germany*

<sup>4</sup>*CNRS, CSNSM, IN2P3, F-91405 Orsay, France*

<sup>5</sup>*School of Physics and Astronomy, The University of Birmingham, Birmingham B15 2TT, United Kingdom*

<sup>6</sup>*GSI Helmholtzzentrum für Schwerionenforschung GmbH, D-64291 Darmstadt, Germany*

<sup>7</sup>*Department of Physics, Post Office Box 3000, University of Oulu, FIN-90014 Oulu, Finland*

<sup>8</sup>*Institut für Kernchemie, Johannes Gutenberg-Universität Mainz, D-55128 Mainz, Germany*

<sup>9</sup>*Department of Physics, University of Jyväskylä, FIN-40014 Jyväskylä, Finland*

<sup>10</sup>*Helsinki Institute of Physics, University of Helsinki, FIN-00014 Helsinki, Finland*

<sup>11</sup>*Physics Department, CERN, CH-1211 Geneva 23, Switzerland*

<sup>12</sup>*Department of Physics, New York University, New York, New York 10003, USA*

(Received 28 September 2010; published 11 November 2010)

Collinear laser spectroscopy was performed on the  $^{80}\text{Ga}$  isotope at ISOLDE, CERN. A low-lying isomeric state with a half-life much greater than 200 ms was discovered. The nuclear spins and moments of the ground and isomeric states and the isomer shift are discussed. Probable spins and parities are assigned to both long-lived states ( $3^-$  and  $6^-$ ) deduced from a comparison of the measured moments to shell-model calculations.

DOI: [10.1103/PhysRevC.82.051302](https://doi.org/10.1103/PhysRevC.82.051302)

PACS number(s): 21.10.Tg, 21.10.Ky, 23.35.+g, 42.62.Fi

Laser spectroscopy is a well-established tool for the model-independent study of nuclear mean-square charge radii, moments and measurements of nuclear spin [1]. In addition, laser spectroscopy is able to reveal new nuclear states and provide unequivocal element (and mass) identification. This includes states that are too long-lived for decay spectroscopy methods or too short-lived for quasi-stable samples to be prepared and analyzed. Collinear laser spectroscopy is essentially limited only by the requirement to produce a beam of sufficient flux.

This article reports optical measurements of  $^{80}\text{Ga}$  ( $Z = 31$ ,  $N = 49$ ). Almost all of the  $N = 49$  isotones have isomeric states with large spin differences compared with the ground states (gs's). In the case of  $^{80}\text{Ga}$ , no such isomeric state has been discovered until now. However, isomeric states can be masked by the gs in  $\beta$ -decay studies if the half-lives are comparable. Hoff and Fogelberg [2] measured  $\gamma$  rays in  $^{80}\text{Ge}$ , produced from the  $\beta$  decay of  $^{80}\text{Ga}$ . A comparison of these  $\gamma$  intensities was made using  $^{80}\text{Ga}$  produced in a fission source and  $^{80}\text{Ga}$  produced in the  $\beta$  decay of  $^{80}\text{Zn}(0^+)$ . In the latter, only low-spin states in Ga are populated. Similar relative  $\gamma$  intensities were observed from both Ga samples, leading to the conclusion that no  $\beta$ -decaying isomeric state existed in  $^{80}\text{Ga}$ . Makishima *et al.* [3] later assigned a spin and parity of  $8^+$  to the 3446-keV nanosecond isomeric state in  $^{80}\text{Ge}$ . The feeding of this high-spin level through the  $^{80}\text{Ga}$   $\beta$  decay implies the existence of a high-spin isomer in  $^{80}\text{Ga}$ . A recent Penning trap mass measurement at JYFL, Jyväskylä, Finland, where  $^{80}\text{Ga}$  isotopes were produced in a proton-induced fission

reaction on a thin target, found no indication of such a state [4].

Collinear laser spectroscopy of gallium isotopes was recently performed [5] at ISOLDE, CERN, revealing an inversion of gs spin between  $^{79}\text{Ga}$  ( $I = 3/2$ ) and  $^{81}\text{Ga}$  ( $I = 5/2$ ). From the measured magnetic moments it was concluded that both gs wave functions are dominated by three protons in the  $\pi f_{5/2}$  level. Thus the low-level structure of  $^{80}\text{Ga}$  will be dominated by the  $\nu g_{9/2}$  hole coupled to this configuration.

Neutron-rich isotopes of Ga were produced in a thick uranium carbide target. After diffusion out of the target, they were extracted as a 30-keV ionic beam and mass-separated using the high-resolution separator. Selective enhancement of the Ga yield by a factor of  $\sim 100$  was provided by the resonance ionization laser ion source (RILIS) [6] using excitation of both the atomic gs and the low-lying metastable state at  $826.24\text{ cm}^{-1}$  (each with an  $\sim 50\%$  thermal population). A proton-neutron converter [7] was used to substantially suppress production of the neutron-deficient Rb isobars, which would otherwise have saturated the trapping volume of the ion beam cooler/buncher ISCOOL [8,9]. In ISCOOL the ions were accumulated for 50 ms up to 200 ms and subsequently released in a bunch of 6- $\mu\text{s}$  temporal length. This bunched  $^{80}\text{Ga}$  beam was overlapped with a copropagating laser beam in the COLLAPS beam line, inducing resonant excitation of the hfs levels. Fluorescent photons were counted only when the Ga pulse passed in front of the photomultiplier tubes, enabling the nonresonant scattered photons from the laser light to be suppressed by a factor of  $3 \times 10^4$ . A Doppler tuning potential was applied to the ion beam (prior to neutralization to the atomic state with Na vapor) for scanning the hyperfine structure (hfs). During this work [5], the optical spectrum of

\*bradley.cheal@manchester.ac.uk

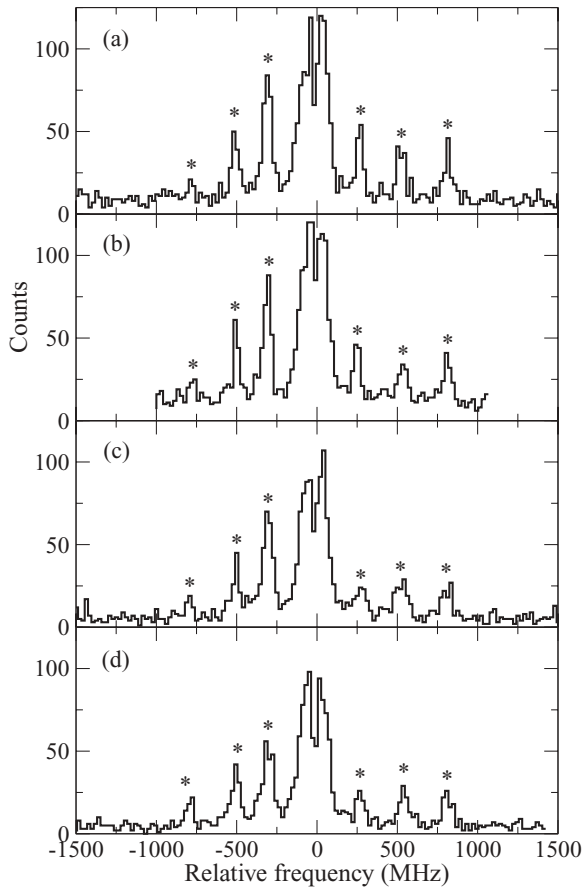


FIG. 1. Optical spectra for  $^{80}\text{Ga}$ , measured on the 417.3-nm  $4p^2P_{3/2} \rightarrow 5s^2S_{1/2}$  line. Four separate scans were taken in this work. Ions were accumulated in the cooler for (a, b) 50 ms or (c, d) 200 ms before release. Asterisks denote the six resolved hyperfine peaks of the wide structure, related to one nuclear state.

$^{80}\text{Ga}$  (the isotope lying at the critical point of the spin inversion) was measured.

Four separate scans were taken of the 417.3-nm  $4p^2P_{3/2} \rightarrow 5s^2S_{1/2}$  atomic line and these are shown in Fig. 1. Owing to the selection rules for this transition, at most six hfs peaks can occur in the spectrum for one nuclear state. The spectra shown in Fig. 1 clearly have contributions from two nuclear states, with the asterisks denoting the six resolved peaks corresponding to the frequency pattern for a single nuclear

state. From the selection rules and number of hfs peaks, this state must have a nuclear spin greater than  $I = 1$ . Likewise, the central structure is from a nuclear state of nonzero spin, for which the hfs peaks are not resolved.

Both nuclear states must arise from  $^{80}\text{Ga}$ , as the signals are produced by resonant collinear laser-atom interaction with a frequency typical for Ga. Of the elements that have a known  $A = 80$  isotope, only Zr and Y have transitions within 1 THz of the 417.3-nm line. Neither would have a measurable production from ISOLDE with the proton-neutron converter in use, and the closest transition is 361 GHz away. Even if an untabulated (and unaccounted for) transition were to exist in another element, it would not be of sufficient strength to match the transition in Ga, the yield of which was enhanced by a factor of  $\sim 100$  using RILIS. Moreover, the relative intensities of the two structures remained invariant with the RILIS yield enhancement factor, which used other transitions characteristic of Ga. It can therefore be unambiguously stated that a low-lying isomeric state exists in  $^{80}\text{Ga}$ , the half-life of which must be much greater than 200 ms, as increasing the cooler accumulation time from 50 to 200 ms did not affect the relative intensities of the two hfs's.

Full hfs's were fitted to the data using a  $\chi^2$ -minimization technique yielding the isomer shift, magnetic hfs constants [ $A = \mu B(0)/I J h$ ] and the quadrupole hfs constants ( $B = e Q_s V_{zz}/h$ ) of the  $^2P_{3/2}$  level. For both structures, the magnetic hfs constant for the upper,  $^2S_{1/2}$ , state was constrained to be  $5.592 \times A(^2P_{3/2})$ , the ratio having been determined from the other measured isotopes [5]. Relative hfs peak intensities for the other Ga isotopes were found to follow a Racah intensity distribution (arising from weak-field angular momentum coupling), which was therefore used to constrain the fit. Full hfs's were fitted to all four data sets simultaneously, with the gs and isomer hfs constants and isomer shift constrained to each be the same for all four sets. For each hfs a comparison of the  $\chi^2$  was made with different values assumed for the nuclear spin.

Table I lists the hfs constants and extracted moments deduced from a fit to the multiplet with the six resolved peaks for alternative spin assignments. A preference is seen for spin  $I = 3$ . This is in agreement with the works of Hoff and Fogelberg [2] and Wingerby *et al.* [10], who proposed a spin 3 for the  $^{80}\text{Ga}$   $\beta$ -decaying state (suggested to be the gs).

For the central structure, the peaks are not fully resolved and the situation is more complicated. Figure 2 shows a

TABLE I. Wide structure hfs coefficients of the  $4s^24p^2P_{3/2}$  level from analysis of the six resolved peaks. Moments are given for each nuclear spin assumed, together with the  $\chi^2$  and the  $\chi^2$  per degree of freedom,  $\chi_r^2$ . Magnetic dipole and spectroscopic electric quadrupole moments are also listed, calibrated using the values for  $^{71}\text{Ga}$  from Refs. [5], [11], and [12].

$I$	$A(^2P_{3/2})$	$B(^2P_{3/2})(\text{MHz})$	$\chi^2(\text{MHz})$	$\chi_r^2$	$\mu(\mu_N)$	$Q_s(\text{b})$
2	-96.37(0.31)	+132.2(3.5)	1009.6	1.61	-1.356(6)	+0.363(21)
<b>3</b>	<b>-67.52(0.14)</b>	<b>+136.5(2.5)</b>	<b>718.5</b>	<b>1.15</b>	<b>-1.425(5)</b>	<b>+0.375(21)</b>
4	-52.15(0.11)	+132.6(2.8)	762.1	1.22	-1.468(5)	+0.364(20)
5	-42.47(0.10)	+126.8(3.3)	849.2	1.36	-1.494(6)	+0.348(20)

TABLE II. Central structure hfs coefficients of the  $4s^2 4p^2 P_{3/2}$  level for different assumed values of nuclear spin, together with the  $\chi^2$  and  $\chi_r^2$ . Nuclear moments are also listed, calibrated using values for  $^{71}\text{Ga}$  from Refs. [5,11], and [12]. The isomer shift,  $\delta\nu^{w,c} = \nu^c - \nu^w$ , is also listed (giving the centroid of the central structure with respect to the wide structure, which is assumed to have  $I = 3$ ). The process is repeated for four minima in the  $\chi^2$  surface. A correction of  $-2.1$  or  $-4.0$  MHz should be added to the isomer shift if the spin of the wide structure is  $I = 4$  or  $I = 5$ , respectively.

$I$	$A(^2P_{3/2})$ (MHz)	$B(^2P_{3/2})$ (MHz)	$\delta\nu^{w,c}$	$\chi^2$	$\chi_r^2$	$\mu$ ( $\mu_N$ )	$Q_s$ (b)
1	+18.14(0.46)	-3.0(2.0)	+3.8(1.9)	878.0	1.40	+0.128(3)	-0.008(6)
2	+10.91(0.24)	-5.2(2.7)	-0.6(1.7)	780.2	1.25	+0.153(3)	-0.014(7)
3	+7.80(0.17)	-7.3(3.1)	-2.4(1.7)	748.9	1.20	+0.165(4)	-0.020(9)
4	+6.07(0.13)	-9.0(3.4)	-3.4(1.6)	734.6	1.17	+0.171(4)	-0.025(9)
5	+4.97(0.10)	-10.3(3.6)	-4.0(1.6)	726.7	1.16	+0.175(4)	-0.028(10)
6	+4.20(0.08)	-11.3(3.8)	-4.5(1.6)	721.8	1.15	+0.177(4)	-0.031(11)
7	+3.64(0.07)	-12.1(3.9)	-4.8(1.6)	718.5	1.15	+0.179(4)	-0.033(11)
8	+3.21(0.06)	-12.7(4.0)	-5.1(1.6)	716.2	1.14	+0.181(4)	-0.035(11)
9	+2.87(0.06)	-13.2(4.1)	-5.3(1.6)	714.4	1.14	+0.182(4)	-0.036(11)
1	-17.43(0.39)	-11.4(3.1)	-15.4(1.7)	824.5	1.32	-0.123(3)	-0.031(9)
2	-10.62(0.21)	-14.2(3.2)	-12.2(1.6)	736.8	1.18	-0.149(3)	-0.039(9)
3	-7.64(0.15)	-16.0(3.4)	-10.8(1.6)	714.1	1.14	-0.161(3)	-0.044(10)
4	-5.97(0.12)	-17.0(3.7)	-10.0(1.6)	706.0	1.13	-0.168(3)	-0.047(10)
5	-4.89(0.09)	-17.6(3.9)	-9.5(1.6)	702.6	1.12	-0.172(3)	-0.048(11)
6	-4.15(0.08)	-17.9(4.0)	-9.1(1.6)	701.1	1.12	-0.175(3)	-0.049(11)
7	-3.60(0.07)	-18.1(4.1)	-8.8(1.6)	700.3	1.12	-0.177(3)	-0.050(12)
8	-3.18(0.06)	-18.2(4.2)	-8.6(1.6)	700.0	1.12	-0.179(3)	-0.050(12)
9	-2.85(0.05)	-18.3(4.3)	-8.5(1.6)	699.8	1.12	-0.180(3)	-0.050(12)
1	-1.92(0.60)	+66.6(1.5)	-15.7(1.7)	826.2	1.32	-0.014(4)	+0.183(10)
2	-2.56(0.33)	+112.2(2.8)	-11.5(2.3)	849.9	1.36	-0.036(5)	+0.308(18)
3	-0.79(3.50)	+142.0(2.9)	-7.8(1.8)	748.9	1.20	-0.017(74)	+0.390(22)
4	+0.58(0.17)	+158.6(3.0)	-7.0(1.6)	719.4	1.15	+0.016(5)	+0.435(24)
5	+0.83(0.12)	+168.2(3.2)	-7.0(1.6)	716.5	1.14	+0.029(4)	+0.462(26)
<b>6</b>	<b>+0.86(0.09)</b>	<b>+174.3(3.4)</b>	<b>-7.1(1.7)</b>	<b>720.1</b>	<b>1.15</b>	<b>+0.036(4)</b>	<b>+0.478(27)</b>
7	+0.82(0.07)	+178.5(3.5)	-7.2(1.7)	725.6	1.16	+0.040(4)	+0.490(27)
8	+0.76(0.06)	+181.6(3.7)	-7.3(1.7)	731.2	1.17	+0.043(4)	+0.498(28)
9	+0.70(0.06)	+184.1(3.8)	-7.4(1.7)	736.4	1.18	+0.044(4)	+0.505(28)
1	+4.67(0.47)	-66.3(1.7)	+4.1(1.9)	888.1	1.42	+0.033(3)	-0.182(11)
2	+3.92(0.27)	-113.6(3.0)	-3.2(1.8)	794.9	1.27	+0.055(4)	-0.312(18)
3	+1.32(0.21)	-145.7(3.1)	-6.7(1.7)	718.0	1.15	+0.028(4)	-0.400(23)
4	-0.04(0.40)	-160.9(3.4)	-7.4(1.6)	725.2	1.16	-0.001(11)	-0.441(25)
5	-0.90(0.14)	-170.4(3.3)	-7.5(1.6)	723.0	1.15	-0.032(5)	-0.467(26)
6	-0.99(0.09)	-176.0(3.3)	-7.4(1.6)	713.8	1.14	-0.042(4)	-0.483(27)
7	-0.95(0.07)	-180.2(3.4)	-7.3(1.6)	707.6	1.13	-0.047(3)	-0.494(27)
8	-0.89(0.06)	-183.4(3.4)	-7.3(1.5)	704.0	1.12	-0.050(3)	-0.503(28)
9	-0.82(0.05)	-186.0(3.4)	-7.3(1.5)	702.0	1.12	-0.052(3)	-0.510(28)

plot of the  $\chi^2$  per degree of freedom as a function of the hyperfine constants for the central structure. Four distinct minima can be seen, showing that the splitting into the two

(symmetrical) groups can be reproduced with a small (positive or negative) magnetic moment or, alternatively, a (positive or negative) quadrupole moment in each case. These four groups

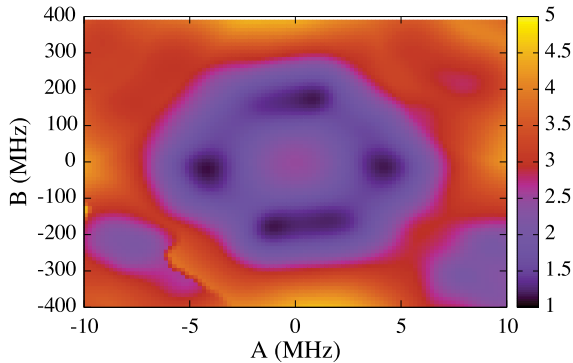


FIG. 2. (Color online) A plot of  $\chi^2$  per degree of freedom as a function of the hfs factors,  $A$  and  $B$ , for the central structure (assuming  $I = 6$ ). All other parameters are minimized for each coordinate.

of solutions, with different values of assumed nuclear spin, are listed in Table II, together with the extracted nuclear moments in each case. Regardless of the nuclear spin, the following restrictions may be placed on the nuclear moments. Either (I)  $0.123\mu_N < |\mu| < 0.182(4)\mu_N$  and  $|Q_s| < 0.050(12)$  b or (II)  $0.182(11)$  b  $< |Q_s| < 0.510(28)$  b and  $|\mu| < 0.055(4)\mu_N$ . Furthermore, irrespective of the assumed spin, we find an isomer shift that is below 16 MHz.

An estimate of the atomic field factor  $F = +410$  MHz fm $^{-2}$  was made using multiconfigurational Dirac-Fock calculations, based on the GRASP92 [13] and RATIP [14] codes. This suggests that the mean-square charge radius of the ground and isomeric states are within 0.04 fm $^2$  of each other. Such a similarity in charge radius may indicate that the isomeric state and the gs have similar structures (at least, similar deformations). Thus the second option is the most likely, because the first option would correspond to a deformation much smaller than that of the wide structure, despite having a similar charge radius.

Calculations by Honma *et al.* [15], using the JUN45 interaction, indeed predicted a multiplet of states with respective spins and parities of  $6^-$ ,  $3^-$ ,  $4^-$ , and  $5^-$ , all within 200 keV (Fig. 36 in Ref. [15]). Considering the small energy difference between the calculated  $6^-$  gs and the first excited  $3^-$  level, these are good candidates for being our long-lived states observed in the two hfs multiplets. From our data it is not possible, however, to determine which of the observed structures is isomeric and which is the gs. Note the similarity of this structure to that of  $^{70}\text{Cu}$  [16], which has one neutron particle in  $\nu g_{9/2}$  coupled to one proton in the  $\pi(pf)$  orbits. Also, in this isotope, the lowest two levels have spins of  $6^-$  and  $3^-$ , separated by about 100 keV, and with a similar  $\beta$ -decay half-life for the isomer and gs, of the order of many seconds. The ordering of these levels could be established only by combining in-source laser spectroscopy with high-precision mass measurements at ISOLTRAP [17]. In a high-precision mass measurement on  $^{80}\text{Ga}$  [4], no signature of an isomeric state was observed suggesting that both levels in  $^{80}\text{Ga}$  must be within about 50 keV, the mass resolving power obtained in that measurement [18].

To gain further insight into the possible structure of the observed isomer and gs, we performed shell-model calculations starting from a  $^{56}\text{Ni}$  core and using the jj44b interaction (as used also in Ref. [5] for odd-Ga isotopes) with the NushellX code. With  $N = 49$  neutrons, the low-lying structure of  $^{80}\text{Ga}$  will be dominated by a  $\nu 1g_{9/2}^{-1}$  hole configuration. This will couple to an odd proton that resides in either the  $\pi f_{5/2}$  or the  $\pi p_{3/2}$  orbit, with the former being more likely, considering that both odd-Ga neighbours are dominated by three protons in  $\pi f_{5/2}$  [5]. We therefore performed restricted shell-model calculations assuming different proton configurations [Figs. 3(a)–3(c)] as well as an unrestricted calculation with protons and neutrons allowed in the  $fpg$  space [excluding  $f_{7/2}$ ; Fig. 3(d)]. In each calculation, a low-lying multiplet of states is observed with spins  $(3,4,5,6)^-$ , but the ordering of these levels changes depending on the chosen proton model space. In all cases except when restricting the space to  $\pi p_{3/2} \otimes \nu g_{9/2}$ , the gs is predicted to be the  $I^\pi = 6^-$  state. Using an unrestricted space, the  $3^-$  state lies at 255 keV, but with a  $5^-$  state 34 keV below. With this level ordering, the  $3^-$  state would be too short-lived to be the isomeric state observed in our experiment. If, instead, the  $3^-$  level lies below the  $5^-$  level, a Weisskopf estimate of the lifetime would be  $>2.73$  s and consistent with our observations, forming a  $\beta$ -decaying isomer.

Predictions for the nuclear moments were made from the shell-model wave functions using the effective charges  $e_p^{\text{eff}} = +1.5e$ ,  $e_n^{\text{eff}} = +1.1e$ , and  $g_s^{\text{eff}} = +0.7g_s^{\text{free}}$  for the effective  $g$  factors. These moments are listed in Table III for the state that lies lowest in energy for the given spin. As expected from the  $\chi^2$  analysis, a spin  $I = 3$  assignment gives the highest consistency between shell-model and experimental moments. For the other structure, assuming spin  $I = 6$ , the estimated quadrupole moment matches well the prolate deformed spin  $I = 6$  quadrupole moment of  $+0.478(27)$  b. For this spin assumption, both the theoretical and the experimental magnetic moments are small and positive, and only a small change in the mixing of the wave functions would be sufficient to ensure full agreement. A poorer consistency is observed between experimental and theoretical moments for spins  $I = 4, 5, 7$ , adding further confidence to spins  $I = 6$  and  $I = 3$  for the two long-lived states. Although the shell model predicts that the  $I = 4$  and  $I = 5$  levels will have a similar

TABLE III. Shell-model calculations of nuclear moments using an unrestricted  $fpg$  model space. Moments are given for the lowest-lying state with the given spin and parity. Experimental moments are taken from Table I for  $I = 3, 4, 5$  and from Table II (third section) for  $I = 6, 7$ .

$I^\pi$	$\mu^{\text{SM}} (\mu_N)$	$Q_s^{\text{SM}} (\text{b})$	$\mu^{\text{expt}} (\mu_N)$	$Q_s^{\text{expt}} (\text{b})$
$3^-$	<b>-1.684</b>	<b>+0.360</b>	<b>-1.425(5)</b>	<b>+0.375(21)</b>
$4^-$	-0.896	+0.156	-1.468(5)	+0.364(20)
$5^-$	+0.405	+0.405	-1.494(6)	+0.348(20)
<b><math>6^-</math></b>	<b>+0.114</b>	<b>+0.508</b>	<b>+0.036(4)</b>	<b>+0.478(27)</b>
$7^-$	+0.968	+0.306	+0.040(4)	+0.490(27)

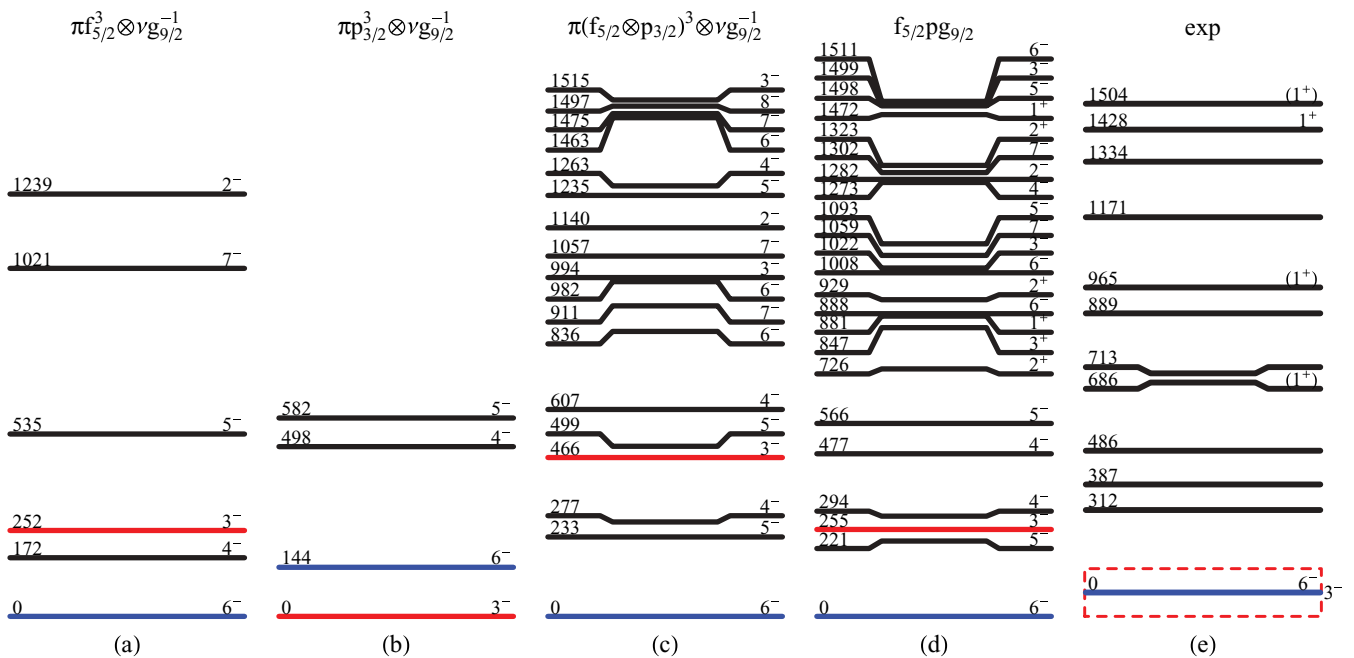


FIG. 3. (Color online) Energy levels (keV) in  $^{80}\text{Ga}$  predicted by shell-model calculations in restricted (a–c) and full (d)  $pfg$  model space with a  $^{56}\text{Ni}$  core, compared to experimental levels (e). Experimental levels are taken from Ref. [19] and this work.

excitation energy, the moments correspond to a hfs too wide to be concealed within the central structure.

In summary, the hyperfine structures of two nuclear states were measured in  $^{80}\text{Ga}$ , unambiguously establishing the existence of a low-lying isomer with a half-life much greater than 200 ms. One of the structures is assigned  $I = 3$  from model-independent analysis of the data alone. Shell-model calculations suggest that the other state is spin  $I = 6$  and that it is the gs. Further Penning trap mass measurements and complementary studies are suggested to determine experimentally which of the two states is the isomeric state and to measure properties such as the excitation energy and half-life.

This work was supported by the German Ministry for Education and Research (BMBF) under Contract No. 06MZ91781, the Helmholtz Association of German Research Centres (Grant Nos. VH-NG-037 and VH-NG-148), the Max-Planck Society, the EU Sixth Framework through Eurons-506065, BriX Research Program No. P6/23, FWO-Vlaanderen (Belgium), and the Science and Technology Facilities Council (UK). E.M. was supported by Conselho Nacional de Desenvolvimento Científico e Tecnológico (CNPq); S.F., by the FiDiPro program of the Finnish Academy; and M.K., by the EU (Grant No MEIF-CT-2006-042114). We also thank the ISOLDE technical group for their support and assistance.

[1] K. T. Flanagan *et al.*, *Phys. Rev. Lett.* **103**, 142501 (2009).  
 [2] P. Hoff and B. Fogelberg, *Nucl. Phys. A* **368**, 210 (1981).  
 [3] A. Makishima *et al.*, *Phys. Rev. C* **59**, 2331(R) (1999).  
 [4] J. Hakala *et al.*, *Phys. Rev. Lett.* **101**, 052502 (2008).  
 [5] B. Cheal *et al.*, *Phys. Rev. Lett.* **104**, 252502 (2010).  
 [6] B. A. Marsh *et al.*, *Hyperfine Interact.* **196**, 129 (2010).  
 [7] U. Köster *et al.*, *Nucl. Instrum. Methods Phys. Res. B* **266**, 4229 (2008).  
 [8] H. Franberg *et al.*, *Nucl. Instrum. Methods Phys. Res. B* **266**, 4502 (2008).  
 [9] E. Mané *et al.*, *Eur. Phys. J. A* **42**, 503 (2009).  
 [10] J. A. Winger *et al.*, *Phys. Rev. C* **36**, 758 (1987).

[11] N. J. Stone, *At. Data Nucl. Data Tables* **90**, 75 (2005).  
 [12] P. Pyykko, *Mol. Phys.* **106**, 1965 (2008).  
 [13] F. A. Parpia, C. F. Fischer, and I. P. Grant, *Comput. Phys. Commun.* **94**, 249 (1996).  
 [14] S. Fritzsche, *J. Electron Spectrosc. Relat. Phenom.* **114-116**, 1155 (2001).  
 [15] M. Honma, T. Otsuka, T. Mizusaki, and M. Hjorth-Jensen, *Phys. Rev. C* **80**, 064323 (2009).  
 [16] J. Van Roosbroeck *et al.*, *Phys. Rev. Lett.* **92**, 112501 (2004).  
 [17] M. Mukherjee *et al.*, *Eur. Phys. J. A* **35**, 31 (2008).  
 [18] J. Hakala and T. Eronen (private communication).  
 [19] B. Singh, *Nucl. Data Sheets* **105**, 223 (2005).